

Research Article

Fullerene C₆₀ Nanotubes Fabricated with Light Irradiation as a Critical Influence Factor

Yongtao Qu,^{1,2} Wenwen Yu,^{1,2} Nana Niu,^{1,2} Shaocen Liang,^{1,2} Guibao Li,^{1,2}
and Guangzhe Piao^{1,2}

¹Key Laboratory of Rubber-Plastics, Ministry of Education, Qingdao University of Science and Technology,
53 Zhengzhou Road, Qingdao, Shandong 266042, China

²School of Polymer Science and Engineering, Qingdao University of Science and Technology, 53 Zhengzhou Road, Qingdao,
Shandong 266042, China

Correspondence should be addressed to Guangzhe Piao, piao@qust.edu.cn

Received 3 August 2012; Accepted 21 August 2012

Academic Editors: V. Kochereshko and S. Krukowski

Copyright © 2012 Yongtao Qu et al. This is an open access article distributed under the Creative Commons Attribution License, which permits unrestricted use, distribution, and reproduction in any medium, provided the original work is properly cited.

Crystalline fullerene C₆₀ nanotubes were prepared simply via liquid-liquid interfacial precipitation using the mixture of C₆₀-saturated pyridine and isopropyl alcohol. C₆₀-saturated pyridine solution was exposed to visible light to promote the growth of fullerene C₆₀ nanotubes. The average diameters of the fullerene particles in C₆₀-pyridine colloid solution after irradiation were characterized by dynamic light scattering. After light irradiation, an outer separated layer of pyridine surrounds the fullerene particles because of the charge transfer complexes formation. The mean ratios of inner diameter to outer diameter of fullerene C₆₀ nanotubes fabricated at different irradiation time and wavelength were given in this paper for the first time. On the basis of the relationship between the average diameters of the fullerene particles in C₆₀-pyridine colloid solution and the mean ratio of inner diameter to outer diameter of FNTs fabricated after irradiation, outer separated layer of pyridine surrounding the fullerene particles was supposed to play an important role in the formation process of fullerene C₆₀ nanotubes.

1. Introduction

Since the discovery of carbon nanotube (CNT), one-dimensional (1D) nanometer-scale materials have been extensively studied owing to their unique structures and physical properties, which lead them to a range of potential applications in the field of nanometer-scale devices. C₆₀ is a well-known fullerene prototype, and its zero-dimensional structure has been generally accepted [1]. It has been expected that the 1D tube of C₆₀, prepared via the self-assembly of zero dimensional C₆₀, will possess the novel optoelectronic and magnetic properties. Fullerene C₆₀ nanofibers (FNFs) have been attracting much attention in recent years [2–5] and found a number of potential applications, such as field-effect transistors [6], solar cells [7], fuel cell catalyst carriers [8], and electrodes [9, 10].

Recently, various synthesis methods have been developed for the preparation of fullerene C₆₀ nanotubes (FNTs), such as solution evaporation [2], template technique [3],

surfactant-assisted method [11], and liquid-liquid interfacial precipitation (LLIP) method [12, 13]. Compared to other synthesis methods, the LLIP is simple and financially viable. FNTs can be achieved at room temperature and without the need for catalysts or surfactants. However, the formation mechanism of the FNTs during the simple and easy to operate LLIP is not clear up till now. So far, several possible mechanisms have been proposed, such as “2+2” cycloaddition [5], core dissolution mechanism [14, 15], concentration depletion mechanism [11], and C₆₀-pyridine colloid as a precursor [16].

In this study, we have found that the visible light irradiation before the mixing of C₆₀-saturated pyridine and isopropyl alcohol (IPA) plays an important role in the formation of FNTs. During the irradiation, there is a color change process of C₆₀-saturated pyridine solution. The average diameters of the fullerene particles in C₆₀-saturated pyridine solution would change greatly after the addition of IPA. The mean ratios of inner diameter to outer diameter

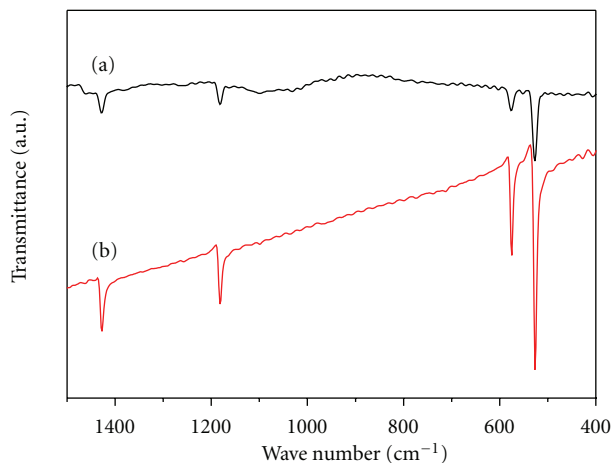


FIGURE 1: FT-IR spectra of FNTs (a), pristine C_{60} powder (b).

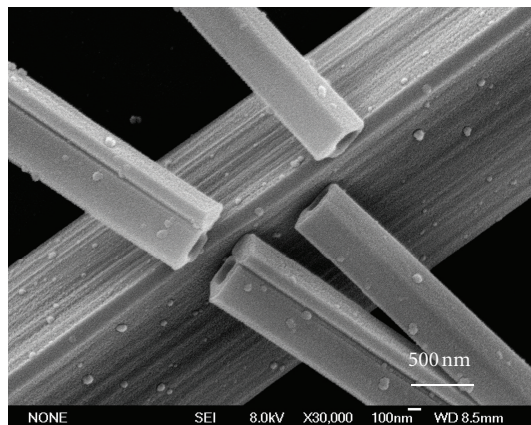
of FNTs depending on the irradiation time were collected in this paper for the first time. On the basis of the relationship between the average diameters of the fullerene particles in C_{60} -pyridine colloid solution and the mean ratios of inner diameter to outer diameter of FNTs fabricated after irradiation, a possible growth mechanism is proposed to describe the formation process of FNTs.

2. Results and Discussion

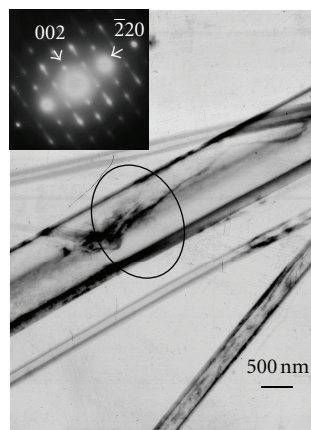
Figure 1 shows FT-IR spectra of FNTs (a) and pristine C_{60} powder (b), respectively. Both spectra showed characteristic sharp absorption peaks of C_{60} (526 , 576 , 1182 , and 1428 cm^{-1}), confirming that the nanotubes are composed of C_{60} molecules [17]. However, as shown in spectra (a), some modifications of the base line were observed even after drying in vacuum, which may be related to the presence of the solvent pyridine or IPA molecules.

The morphology of the FNTs was analyzed by SEM. As shown in Figure 2(a), the FNTs have the fibril structures with the diameter of about 500 nm , and all the cross sections of FNTs have the rectangle structures. Figure 2(b) shows a TEM image of typical FNTs precipitated in the C_{60} -saturated pyridine and IPA colloidal solution. The FNTs show tubular structure with wide size distribution. To accurately analyze outer diameter size distribution of FNTs, the outer diameter of 99 FNTs have been measured and the diameter size distribution is shown in Figure 3. As shown, most FNTs have the outer diameters ranging from 200 nm to 600 nm , accounting for 89% of all samples. The acquired select area electron diffraction (SAED) pattern of an FNT inset in Figure 2(b) indicates that the FNT is a local single crystal.

To confirm the crystal structure of FNTs, XRD analysis was carried out and the XRD pattern of the FNTs is shown in Figure 4. There are five diffraction peaks, which have been indexed as the (111), (220), (311), (420), and (511) diffraction peaks from an fcc lattice, indicating that the FNTs have a face-centered cubic (fcc) structure with cell dimensions $a = 1.402 \pm 0.002$. From the SAED pattern, the



(a)



(b)

FIGURE 2: (a) SEM image of FNTs; (b) TEM image of FNTs. Inset in (b) is a SAED pattern of enclosed part indicating the tube wall is local single crystalline.

growth direction of the FNT is $[110]$, which is in good agreement with the result reported by Minato et al. [18].

In the process of preparing FNTs, it is found that the freshly prepared C_{60} -pyridine solution is purple-pinkish at the beginning but turns into burgundy over time [19]. Interestingly, the visible light irradiation such as green light centered at 525 nm can speed up the color change process if the C_{60} -pyridine solution is exposed to visible light. However, such color change is not observed in the C_{60} -toluene or C_{60} -*m*-xylene solution [20, 21]. The color change of C_{60} -pyridine solution depending on the irradiation time was recorded by using the UV-visible spectrophotometer (Figure 5).

As shown in Figure 5 (a-c), after light irradiation, the characteristic valley of C_{60} located at about 440 nm in the C_{60} spectrum [22] progressively disappears with increasing irradiation time. After light irradiation, the absorbance of the freshly prepared purple-pinkish solution (trace a) increases visibly in the region of $400\text{--}500\text{ nm}$ (trace b-c), which is consistent with the observed color change. But when the irradiation time increases to 50 min , the absorption in the region of $400\text{--}500\text{ nm}$ decreases (trace d) visibly compared

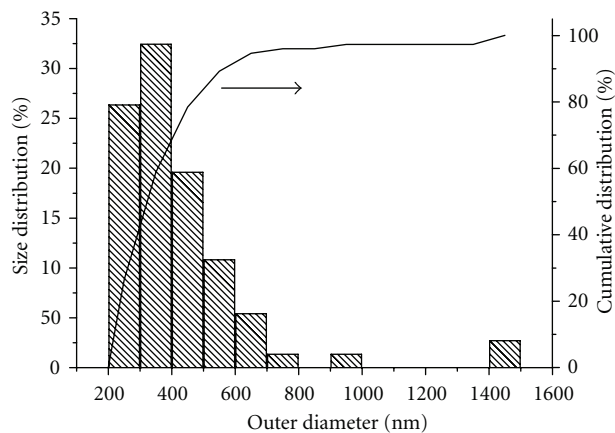


FIGURE 3: Size distribution of outer diameter of FNTs.

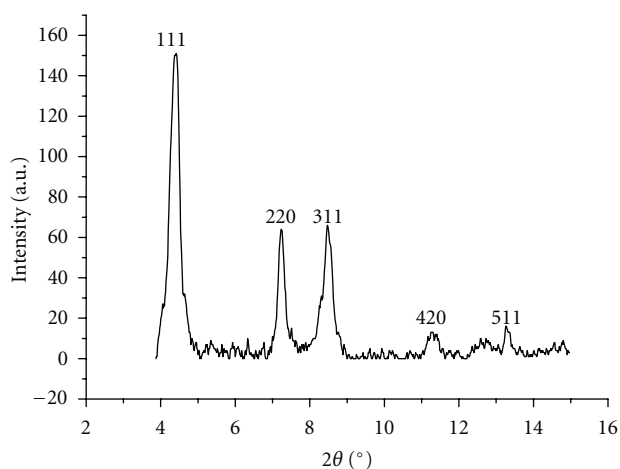


FIGURE 4: XRD pattern of FNTs.

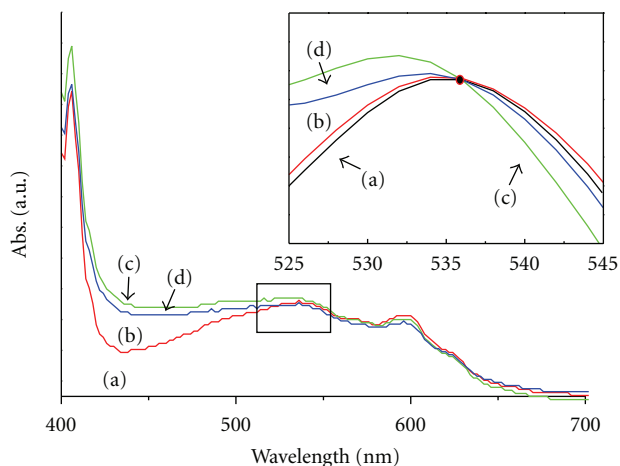


FIGURE 5: UV-vis absorption spectra of C_{60} -pyridine solution. Freshly prepared purple-pinkish solution (a), burgundy solution irradiated by green light (525 nm) for different time (b) 5 min, (c) 30 min, (d) 60 min. The inset shows the details of the spectral structure in the 520–550 nm wavelength region.

with trace c. The inset shows the details of the spectral structure in the 520–550 nm wavelength region, where an intersection point of trace a–d take place at about 536 nm. This intersection point is defined as the isoabsorptive point. The existence of isoabsorptive point means a balanced reaction between two substances in the C_{60} -saturated pyridine solution when irradiated by green light.

This phenomenon is probably related to the formation of the C_{60} -pyridine charge transfer (CT) complexes [23, 24]. Fullerene C_{60} has the ability to accept multiple electrons, making it become a potential electron accumulator [24, 25]. On the other hand, pyridine has a nitrogen atom with lone pair, which allows the molecule to be an electron donor [19, 26]. It is reasonable that CT complex should exist in the C_{60} -pyridine system under certain condition. The absorption peak in the region of 400–450 nm corresponds to CT complex absorption, and the characteristic valley located at 440 nm and the absorption in the region of about 500–600 nm are corresponds to C_{60} molecules absorption.

To further understand the color change process, the average diameters of the fullerene particles in C_{60} -saturated pyridine solution were detected by DLS with different irradiation time and the corresponding diameter changes after IPA addition, which are shown in Figure 6.

As shown in Figure 6, the mean diameters of the fullerene particles vary with the irradiation time. Compared to other irradiation time, when irradiated by green light for 30 min, the fullerene particles in C_{60} -saturated pyridine solution show the largest mean diameter about 260 nm. It is speculated that the pristine C_{60} molecules were surrounded by a large amount of pyridine molecules due to the formation of CT complexes. It is supposed that 30 min is the optimum irradiation time to form CT complexes between pyridine and C_{60} molecules according to the UV-vis absorption spectra. So some pyridine molecules may even permeate into the loose pristine C_{60} particles to form CT complexes with C_{60} molecules. Due to pyridine molecules' permeation and CT complexes' formation, the pristine C_{60} particles in the C_{60} -saturated pyridine solution became looser and showed larger diameters. This hypothesis is supported by the mean diameter decrease after IPA injection.

After IPA is added, C_{60} -pyridine colloids will be formed. The mean diameter of C_{60} -pyridine colloids without the irradiation increases significantly to about 1400 nm. If no irradiation, little CT complexes formed. Without the separation of pyridine adsorbed by fullerene molecules around fullerene particles, the fullerene molecules will contact with the polar medium IPA directly, which is energetically unfavorable and they prefer to aggregate [27]. So irradiation plays an important role in the stability of C_{60} -pyridine colloids after IPA injection.

Fullerene particles will not dissolve with the polar solvent IPA because IPA is a bad solvent for fullerenes. However, as shown in Figure 6, the mean diameter of C_{60} -pyridine colloids decreases significantly after IPA injection when the irradiation time is about 20–40 min. This phenomenon may result from the hydrophobic interaction when IPA was injected into C_{60} pyridine solution [28, 29]. Pyridine was adsorbed by fullerene molecules when CT complexes formed

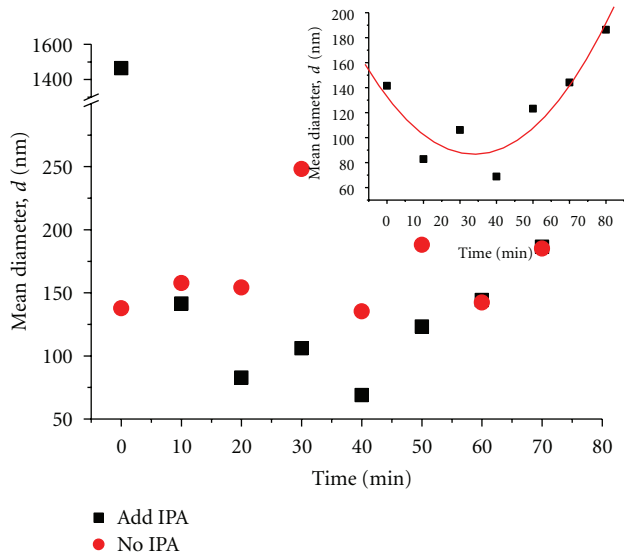


FIGURE 6: Dependence of mean diameters of the fullerene particles on the irradiation time. (■) Mean diameters of C_{60} -saturated pyridine solution; (●) mean diameters of C_{60} -pyridine colloids after IPA added. The inset shows the fitted curve to the mean diameters of C_{60} -pyridine colloids after IPA injection.

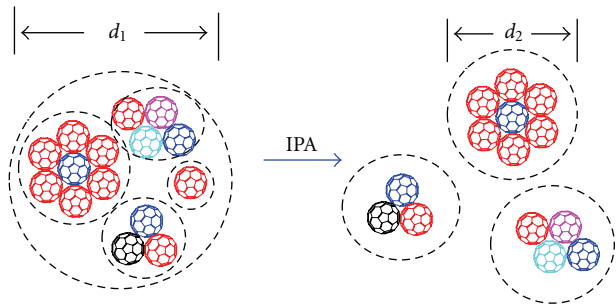


FIGURE 7: Schematic diagram of the size decrease process when IPA injected. (---) Outer separated layer of absorbed pyridine.

appear to act as a surfactant around fullerene molecules protecting them from IPA [11, 30]. So there will be some repulsive interaction between nonpolar Pyridine and polar IPA. Contrarily, there is no aggregation but size decrease ($d_2 < d_1$), as can be seen in Figure 7. The hydrophobic surfactant interactions are thought to act in stabilizing the structures into small-sized sphere-like fullerene particles [31].

Interestingly, there is little size variation when the irradiation time increases to 60–70 min. Just as shown in UV-vis analysis, excessive light irradiation goes against the formation of CT complexes. So the C_{60} particles would also be encapsulated by an outer layer of pyridine, and no aggregation would happen when IPA injected. But there is not enough pyridine adsorbed by fullerene particles, and hydrophobic interaction is not strong enough for the size decrease when irradiated for 60–70 min.

The inset in Figure 6 shows the fitted curve to the mean diameters of C_{60} -pyridine colloids after IPA added. The

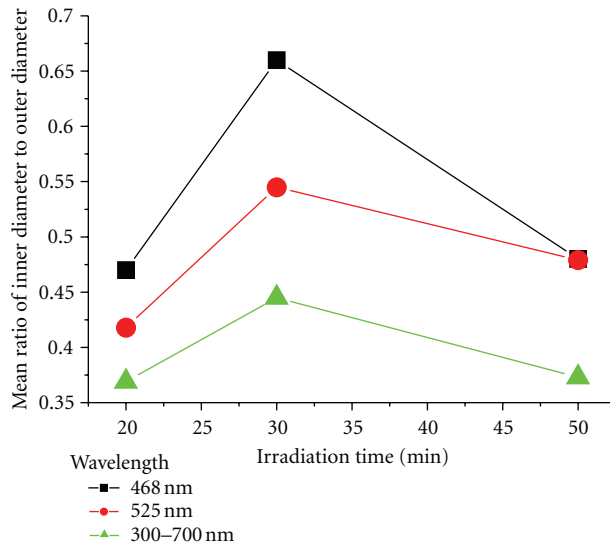


FIGURE 8: Irradiation time and wavelength dependence of the mean ratio of inner diameter to outer diameter of FNTs. (■) Irradiated by blue light centered at 468 nm; (●) irradiated by green light centered at 528 nm; (▲) irradiated by white light in the region of 300–700 nm.

relationship between the irradiation time (x , min) and the mean diameters of the C_{60} -pyridine colloids (y , nm) was fitted by a curve of $y = 0.08x^2 - 5.5x + 179$. The equation suggests that when the irradiation time is 34 min, there are the smallest colloid particles after IPA injected, which means the most stable structure of C_{60} -pyridine colloid.

Figure 8 gives the irradiation time and wavelength dependence of the mean ratio of inner diameter to outer diameter of FNTs.

As shown in Figure 8, when the wavelength of irradiated light centered at 468 nm, the ratio of inner diameter to outer diameter is about 0.67, which is the largest. This is because the increase absorbance of fullerene C_{60} dissolved in pyridine solution within the short light wavelength regions, which is beneficial to the formation of CT complexes [32]. Taking no account of wavelength, when irradiated by 30 min, there is the largest ratio of inner diameter to outer diameter of FNTs, which means relatively largest inner diameter and thinnest tube wall.

With the experimental observations mentioned in the above section, a possible growth mechanism describing the formation process of C_{60} FNTs is proposed. The schematic is shown in Figure 9.

After light irradiation, C_{60} -pyridine CT complexes formed immediately, which play an important role in the nucleation and crystal growth process. Previous works [33, 34] have reported that C_{60} colloids with narrow size distributions were immediately formed when the solution of fullerenes in a good solvent was injected into a poor solvent. So when IPA was injected into C_{60} -saturated pyridine solution, crystal seeds were formed immediately. Besides the crystal seeds, sphere-like fullerene particles were encapsulated by an outer layer of pyridine because of CT

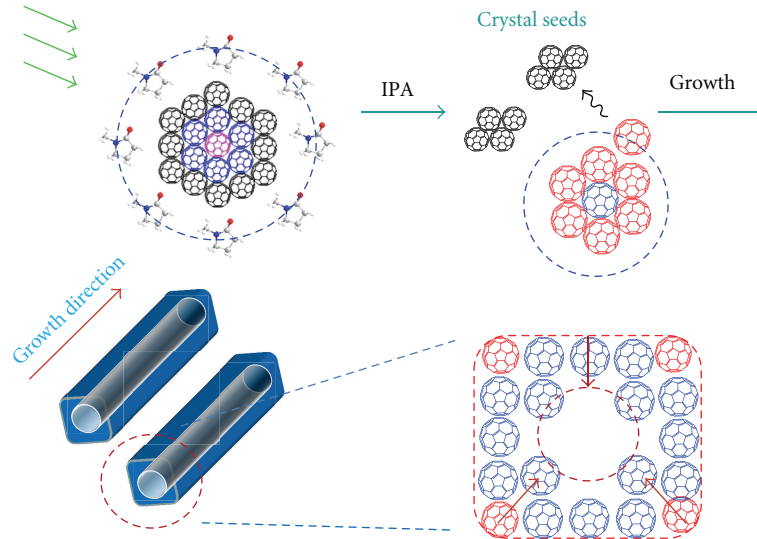


FIGURE 9: Schematic of the formation process of C_{60} FNTs.

complexes formation, which acted as the C_{60} suppliers in the crystal growth process. Due to the highly anisotropic nature of these crystal seeds [27], the growth direction was largely confined to the [110] direction, resulting in one-dimensional structure [35]. During the crystal growth after nucleation, the C_{60} molecules prefer the corners of the rectangle cross section, as indicated by the red C_{60} molecules in Figure 9, because the corner sites have a relatively higher free energy [36]. The secondarily preferable sites for C_{60} molecules are the edges of the cross section, as indicated by the blue molecules. The last ones are the central portion of the cross section, and this crystal growth process will end at the equilibrium point, when the C_{60} suppliers are too stable to supply C_{60} molecules to the central portion [11].

According to this mechanism, it is expected to obtain FNTs with different ratios of inner diameter to outer diameter when the C_{60} suppliers have different equilibrium points. In this study, it is the most favorable condition for the formation of CT complexes between pyridine and C_{60} molecules when the C_{60} -saturated pyridine solution was irradiated by light with relatively short wavelength and optimum time. After IPA injection, the most stabilized sphere-like fullerene particles with smallest diameters encapsulated by an outer layer of pyridine were formed immediately. Reaching to the equilibrium point easily, these stable fullerene particles are not likely to supply C_{60} to the central portion of the tubes because of the outer protect layer of pyridine. As a result, FNTs with relatively thinner walls and clear inner diameters were formed. Some researchers have suggested that the rate of growth of a crystal face is a function of the degree of supersaturation at that face [35, 36]. The protection layer of pyridine outside the fullerene particles extends the duration of the C_{60} supply stage, which means low supersaturation at the face, indicating that the process of increasing the reproducibility of high-quality FNTs with relatively largest inner diameter and thinnest tube wall is rather slow and steady.

3. Experimental Section

FNTs were prepared at ambient pressure and around room temperature using C_{60} fullerene powder (99.5% purity, MER Ltd.) based on the experimental procedures described in references [16, 37]. The typical procedure was as follows. After ultrasonication for 10 min in an ice water bath, a purple-pinkish pyridine solution saturated with C_{60} was prepared. In order to promote the growth of the FNTs, the solution was exposed to visible light such as green light with the center wavelength of 525 nm [20, 32, 38]. After irradiation, the red purple pyridine solution turned into burgundy solution immediately. 2 mL of this brown pyridine solution was put into a transparent 25 mL glass bottle, followed by adding 18 mL of IPA. To obtain suitable diffusion at the interface, the mixture was vigorously agitated in an ultrasonic bath for 1 min before stored at 8°C. Golden-brown cluster fibers were suspended in the solutions after about 12 hours.

Infrared spectroscopy was performed for the specimen dried at room temperature and using an FTIR apparatus (Bruker Vertex 70). Hollow structure of the C_{60} FNTs was characterized by using transmission scanning electron microscope (TEM, JEOL JEM-2000EX) and scanning electron microscope (SEM, JEOL JSM-6700F). For the purpose of electron microscopic measurement, the specimens were placed on silicon wafer substrates or copper microgrid with carbon film. The XRD measurements were performed at Beijing Synchrotron Radiation Facility (BSRF) at ambient temperature. The X-ray wavelength was 0.06199 nm, and the beam size was 25 μm in diameter. The color change of C_{60} -pyridine solution was recorded by using the UV-visible spectrophotometer (SHIMADZU UV-2400PC). The average diameters of the fullerene particles in C_{60} -pyridine colloid solution were detected immediately with DLS (Zetasizer Nano ZS90).

4. Conclusions

Irradiated with optimum time, the FNTs with relatively thinner walls and clear inner diameters were prepared via LLIP using the mixture of C₆₀-saturated pyridine and IPA at 8°C. After light irradiation, C₆₀-pyridine CT complexes formed immediately, which play an important role in the nucleation and crystal growth process. A protection layer of pyridine outside the fullerene particles was formed because of CT complex formation. After IPA injected, stable C₆₀-pyridine colloids will be formed, which acted as the C₆₀ suppliers in the crystal growth process. The hydrophobic surfactant interactions might act in stabilizing the structures into small-sized sphere-like fullerene colloid particles. When the irradiation time was 34 min, there were the smallest particles after IPA injection, which means the most stabilization of C₆₀-pyridine colloid and the topmost reproducibility of high quality FNTs with relatively largest inner diameter and thinnest tube wall. On the basis of experimental observations, a possible growth mechanism is proposed to describe the formation process of C₆₀ FNTs.

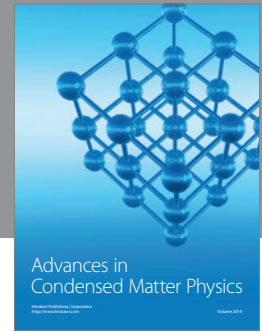
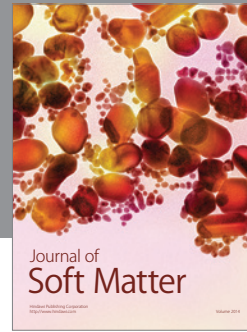
Acknowledgments

This work was partially supported by the Program for International S&T Cooperation Projects in the Ministry of Science and Technology of China (2011DFA50430), National Natural Science Foundation of China (50773033 and 50872060), Science Foundation of Shandong Province (Y2007F01 and Q2008F07), and Doctoral Fund of QUST.

References

- [1] H. W. Kroto, J. R. Heath, S. C. O'Brien, R. F. Curl, and R. E. Smalley, "C₆₀: buckminsterfullerene," *Nature*, vol. 318, no. 6042, pp. 162–163, 1985.
- [2] L. Wang, B. Liu, D. Liu et al., "Synthesis of thin, rectangular C₆₀ nanorods using m-xylene as a shape controller," *Advanced Materials*, vol. 18, no. 14, pp. 1883–1888, 2006.
- [3] H. Liu, Y. Li, L. Jiang et al., "Imaging as-grown [60] fullerene nanotubes by template technique," *Journal of the American Chemical Society*, vol. 124, no. 45, pp. 13370–13371, 2002.
- [4] Y. G. Guo, C. J. Li, L. J. Wan et al., "Well-defined fullerene nanowire arrays," *Advanced Functional Materials*, vol. 13, no. 8, pp. 626–630, 2003.
- [5] K. Miyazawa, Y. Kuwasaki, A. Obayashi, and M. Kuwabara, "C₆₀ nanowhiskers formed by the liquid-liquid interfacial precipitation method," *Journal of Materials Research*, vol. 17, no. 1, pp. 83–88, 2002.
- [6] K. Ogawa, T. Kato, A. Ikegami et al., "Electrical properties of field-effect transistors based on C₆₀ nanowhiskers," *Applied Physics Letters*, vol. 88, no. 11, Article ID 112109, 3 pages, 2006.
- [7] P. R. Somani, S. P. Somani, and M. Umeno, "Toward organic thick film solar cells: three dimensional bulk heterojunction organic thick film solar cell using fullerene single crystal nanorods," *Applied Physics Letters*, vol. 91, no. 17, Article ID 173503, 3 pages, 2007.
- [8] K. Miyazawa, "Synthesis and properties of fullerene nanowhiskers and fullerene nanotubes," *Journal of Nanoscience and Nanotechnology*, vol. 9, no. 1, pp. 41–50, 2009.
- [9] X. Zhang, K. Jiao, G. Piao, S. Liu, and S. Li, "Voltammetric study of fullerene C₆₀ and fullerene C₆₀ nanotubes with sandwich method," *Synthetic Metals*, vol. 159, no. 5–6, pp. 419–423, 2009.
- [10] X. Zhang, Y. Qu, G. Piao, J. Zhao, and K. Jiao, "Reduced working electrode based on fullerene C₆₀ nanotubes@DNA: characterization and application," *Materials Science and Engineering B*, vol. 175, no. 2, pp. 159–163, 2010.
- [11] H. X. Ji, J. S. Hu, Q. X. Tang et al., "Controllable preparation of submicrometer single-crystal C₆₀ rods and tubes through concentration depletion at the surfaces of seeds," *Journal of Physical Chemistry C*, vol. 111, no. 28, pp. 10498–10502, 2007.
- [12] K. Miyazawa, A. Obayashi, and M. Kuwabara, "C₆₀ nanowhiskers in a mixture of lead zirconate titanate sol-C₆₀ toluene solution," *Journal of the American Ceramic Society*, vol. 84, no. 3–12, pp. 3037–3039, 2001.
- [13] J. Y. Hu, N. N. Niu, G. Z. Piao et al., "Phase transitions in single crystal tubes formed from C₆₀ molecules under high pressure," *Carbon*, vol. 50, no. 15, pp. 5458–5462, 2012.
- [14] K. Miyazawa, J. I. Minato, T. Yoshii, M. Fujino, and T. Suga, "Structural characterization of the fullerene nanotubes prepared by the liquid-liquid interfacial precipitation method," *Journal of Materials Research*, vol. 20, no. 3, pp. 688–695, 2005.
- [15] K. Miyazawa, K. Hamamoto, S. Nagata, and T. Suga, "Structural investigation of the C₆₀/C₇₀ whiskers fabricated by forming liquid-liquid interfaces of toluene with dissolved C₆₀/C₇₀ and isopropyl alcohol," *Journal of Materials Research*, vol. 18, no. 5, pp. 1096–1103, 2003.
- [16] G. Li, P. Liu, Z. Han et al., "A novel approach to fabrication of fullerene C₆₀ nanotubes: using C₆₀-pyridine colloid as a precursor," *Materials Letters*, vol. 64, no. 3, pp. 483–485, 2010.
- [17] W. Kratschmer, L. D. Lamb, K. Fostiropoulos, and D. R. Huffman, "Solid C₆₀: a new form of carbon," *Nature*, vol. 347, no. 6291, pp. 354–358, 1990.
- [18] J. I. Minato, K. Miyazawa, and T. Suga, "Morphology of C₆₀ nanotubes fabricated by the liquid-liquid interfacial precipitation method," *Science and Technology of Advanced Materials*, vol. 6, no. 3–4, pp. 272–277, 2005.
- [19] J. X. Cheng, Y. Fang, Q. J. Huang, Y. J. Yan, and X. Y. Li, "Blue-green photoluminescence from pyridine-C₆₀ adduct," *Chemical Physics Letters*, vol. 330, no. 3–4, pp. 262–266, 2000.
- [20] M. Tachibana, K. Kobayashi, T. Uchida, K. Kojima, M. Tanimura, and K. Miyazawa, "Photo-assisted growth and polymerization of C₆₀ "nano" whiskers," *Chemical Physics Letters*, vol. 374, no. 3–4, pp. 279–285, 2003.
- [21] Y. Qu, S. Liang, K. Zou et al., "Effect of solvent type on the formation of tubular fullerene nanofibers," *Materials Letters*, vol. 65, no. 3, pp. 562–564, 2011.
- [22] J. R. Lakowicz, *Principle of Fluorescence Spectroscopy*, Kluwer Academic/Plenum, New York, NY, USA, 2nd edition, 1999.
- [23] H. Imahori, K. Hagiwara, T. Akiyama, S. Taniguchi, T. Okada, and Y. Sakata, "Synthesis and photophysical property of porphyrin-linked fullerene," *Chemistry Letters*, vol. 24, pp. 265–266, 1995.
- [24] D. Kuciauskas, S. Lin, G. R. Seely et al., "Energy and photoinduced electron transfer in porphyrin-fullerene dyads," *Journal of Physical Chemistry*, vol. 100, no. 39, pp. 15926–15932, 1996.
- [25] E. F. Sheka, "Donor-acceptor interaction and fullerene C₆₀ dimerization," *Chemical Physics Letters*, vol. 438, no. 1–3, pp. 119–126, 2007.
- [26] R. Świetlik, P. Byszewski, and E. Kowalska, "Interactions of C₆₀ with organic molecules in solvate crystals studied by infrared

- spectroscopy,” *Chemical Physics Letters*, vol. 254, no. 1-2, pp. 73–78, 1996.
- [27] R. G. Alargova, S. Deguchi, and K. Tsujii, “Stable colloidal dispersions of fullerenes in polar organic solvents,” *Journal of the American Chemical Society*, vol. 123, no. 43, pp. 10460–10467, 2001.
- [28] K. S. Schmitz, *An Introduction to Dynamic Light Scattering by Macromolecules*, Academic Press, San Diego, Calif, USA, 1990.
- [29] R. Pecora, *Dynamic Light Scattering*, Plenum Press, New York, NY, USA, 1985.
- [30] A. Mrzei, A. Mertelj, A. Omerzu, M. Copic, and D. Mihailovic, “Investigation of encapsulation and solvatochromism of fullerenes in binary solvent mixtures,” *Journal of Physical Chemistry B*, vol. 103, no. 51, pp. 11256–11260, 1999.
- [31] G. V. Andrievsky, V. K. Klochkov, A. B. Bordyuh, and G. I. Dovbeshko, “Comparative analysis of two aqueous-colloidal solutions of C_{60} fullerene with help of FTIR reflectance and UV-Vis spectroscopy,” *Chemical Physics Letters*, vol. 364, no. 1-2, pp. 8–17, 2002.
- [32] C. L. Ringor and K. Miyazawa, “Synthesis of C_{60} nanotubes by liquid-liquid interfacial precipitation method: influence of solvent ratio, growth temperature, and light illumination,” *Diamond and Related Materials*, vol. 17, no. 4-5, pp. 529–534, 2008.
- [33] S. Nath, H. Pal, D. K. Palit, A. V. Sapre, and J. P. Mittal, “Aggregation of fullerene, C_{60} , in benzonitrile,” *Journal of Physical Chemistry B*, vol. 102, no. 50, pp. 10158–10164, 1998.
- [34] A. D. Bokare and A. Patnaik, “ C_{60} aggregate structure and geometry in nonpolar o-xylene,” *Journal of Physical Chemistry B*, vol. 109, no. 1, pp. 87–92, 2005.
- [35] B. Mayers and Y. N. Xia, “Formation of tellurium nanotubes through concentration depletion at the surfaces of seeds,” *Advanced Materials*, vol. 14, pp. 279–282, 2002.
- [36] G. C. Krueger and C. W. Miller, “A study in the mechanics of crystal growth from a supersaturated solution,” *The Journal of Chemical Physics*, vol. 21, no. 11, pp. 2018–2023, 1953.
- [37] G. Li, Z. Han, G. Piao, J. Zhao, S. Li, and G. Liu, “To distinguish fullerene C_{60} nanotubes and C_{60} nanowhiskers using Raman spectroscopy,” *Materials Science and Engineering B*, vol. 163, no. 3, pp. 161–164, 2009.
- [38] K. Kobayashi, M. Tachibana, and K. Kojima, “Photo-assisted growth of C_{60} nanowhiskers from solution,” *Journal of Crystal Growth*, vol. 274, no. 3-4, pp. 617–621, 2005.



Hindawi

Submit your manuscripts at
<http://www.hindawi.com>

